Standard Guide for
Assessing Microstructure of Polymeric Scaffolds for Use in Tissue-Engineered Medical Products[1]

1. Scope

1.1 This guide covers an overview of test methods that may be used to obtain information relating to the dimensions of pores, the pore size distribution, the degree of porosity, interconnectivity, and measures of permeability for porous materials used as polymeric scaffolds in the development and manufacture of tissue-engineered medical products (TEMPs). This information is key to optimizing the structure for a particular application, developing robust manufacturing routes, and providing reliable quality control data.

1.2 The values stated in SI units are to be regarded as standard. No other units of measurement are included in this standard.

1.3 *This guide does not purport to address all of the safety concerns, if any, associated with its use. It is the responsibility of the user of this standard to establish appropriate safety and health practices and to determine the applicability of regulatory limitations prior to use.*

2. Referenced Documents

2.1 *ASTM Standards:*[2]

D2873 Test Method for Interior Porosity of Poly(Vinyl Chloride) (PVC) Resins by Mercury Intrusion Porosimetry (Withdrawn 2003)[3]

D4404 Test Method for Determination of Pore Volume and Pore Volume Distribution of Soil and Rock by Mercury Intrusion Porosimetry

E128 Test Method for Maximum Pore Diameter and Permeability of Rigid Porous Filters for Laboratory Use

E1294 Test Method for Pore Size Characteristics of Membrane Filters Using Automated Liquid Porosimeter (Withdrawn 2008)[3]

E1441 Guide for Computed Tomography (CT) Imaging

F316 Test Methods for Pore Size Characteristics of Membrane Filters by Bubble Point and Mean Flow Pore Test

F2150 Guide for Characterization and Testing of Biomaterial Scaffolds Used in Tissue-Engineered Medical Products

F2603 Guide for Interpreting Images of Polymeric Tissue Scaffolds

3. Terminology

3.1 *Definitions:*

3.1.1 *bioactive agent, n*—any molecular component in, on, or within the interstices of a device that is intended to elicit a desired tissue or cell response.

3.1.1.1 *Discussion*—Growth factors and antibiotics are typical examples of bioactive agents. Device structural components or degradation byproducts that evoke limited localized bioactivity are not bioactive agents.

3.1.2 *blind (end)-pore, n*—a pore that is in contact with an exposed internal or external surface through a single orifice smaller than the pore's depth.

3.1.3 *closed cell, n*—a void isolated within a solid, lacking any connectivity with an external surface. Synonym: *closed pore*

3.1.4 *hydrogel, n*—a water-based open network of polymer chains that are cross-linked either chemically or through crystalline junctions or by specific ionic interactions.

3.1.5 *macropore/macroporosity* (life sciences) *, n*—a structure (including void spaces) sized to allow substantially unrestricted passage of chemicals, biomolecules, viruses, bacteria, and mammalian cells. In implants with interconnecting pores, macroporosity provides dimensions that allow for ready tissue penetration and microvascularization after implantation. Includes materials that contain voids with the potential to be observable to the naked eye (>100 µm).

3.1.6 *micropore/microporosity* (life sciences) *, n*—a structure (including void spaces) sized to allow substantially unrestricted passage of chemicals, biomolecules, and viruses while sized to control or moderate the passage of bacteria, mammalian cells, and/or tissue. Includes materials with typical pore

sizes of greater than 0.1 µm (100 nm) and less than about 100 µm (100 000 nm), with a common microporous context encompassing the range of 20 µm or less for the filtration of cells ranging from bacteria to common mammalian cells and above 30 µm for the ingrowth of tissue. Objects in this size range typically can be observed by conventional light microscopy.

3.1.7 *nanopore/nanoporosity (life sciences), n*—a structure inclusive of void spaces sized to control or moderate the passage of chemicals, biomolecules, and viruses while sized to substantially exclude most bacteria and all mammalian cells. Includes materials with typical pore sizes of less than 100 nm (0.1 µm), with common nanoporous context in the range of ~20 nm or less for the filtration of viruses.

3.1.8 *permeability, n*—a measure of fluid, particle, or gas flow through an open pore structure.

3.1.9 *polymer, n*—a long chain molecule composed of monomers including both natural and synthetic materials. Examples include collagen and polycaprolactone.

3.1.10 *pore, n*—a fluid (liquid or gas) filled externally connecting channel, void, or open space within an otherwise solid or gelatinous material (for example, textile meshes composed of many or single fibers (textile based scaffolds), open cell foams, (hydrogels)). Synonyms: *open-pore, through-pore*.

3.1.11 *porogen, n*—a material used to create pores within an inherently solid material.

3.1.11.1 *Discussion*—For example, a polymer dissolved in an organic solvent is poured over a water-soluble powder. After evaporation of the solvent, the porogen is leached out, usually by water, to leave a porous structure. The percentage of porogen needs to be high enough to ensure that all the pores are interconnected.

3.1.12 *porometry, n*—the determination of the distribution of open pore diameters relative to the direction of fluid flow by the displacement of a non-volatile wetting fluid as a function of pressure.

3.1.13 *porosimetry, n*—the determination of the pore volume and pore size distribution through the use of a non-wetting liquid (typically mercury) intrusion into a porous material as a function of pressure.

3.1.14 *porosity, n*—property of a solid which contains an inherent or induced network of channels and open spaces. Porosity can be determined by measuring the ratio of pore (void) volume to the apparent (total) volume of a porous material and is commonly expressed as a percentage.

3.1.15 *scaffold, n*—a support, delivery vehicle, or matrix for facilitating the migration, binding, or transport of cells or bioactive molecules used to replace, repair, or regenerate tissues.

3.1.16 *through-pores, n*—an inherent or induced network of voids or channels that permit flow of fluid (liquid or gas) from one side of the structure to the other.

3.1.17 *tortuosity, n*—a measure of the mean free path length of through-pores relative to the sample thickness. Alternative

definition: The squared ratio of the mean free path to the minimum possible path length.

4. Summary of Guide

4.1 The microstructure, surface chemistry, and surface morphology of polymer-based tissue scaffolds plays a key role in encouraging cell adhesion, migration, growth, and proliferation. The intention of this guide is to provide a compendium of techniques for characterizing this microstructure. The breadth of the techniques described reflects the practical difficulties of quantifying pore sizes and pore size distributions over length scales ranging from nanometres to sub-millimetres and the porosity of materials that differ widely in terms of their mechanical properties.

4.2 These microstructural data when used in conjunction with other characterization methods, for example, chemical analysis of the polymer (to determine parameters such as the molecular weight and its distribution), will aid in the optimization of scaffolds for tissue-engineered medical products (TEMPs). Adequate characterization is also critical to ensure the batch-to-batch consistency of scaffolds; either to assess base materials supplied by different suppliers or to develop robust manufacturing procedures for commercial production.

4.3 Application of the techniques described in this guide will not guarantee that the scaffold will perform the functions for which it is being developed but they may help to identify the reasons for success or failure.

4.4 This guide does not suggest that all listed tests be conducted. The choice of technique will depend on the information that is required and on the scaffold's physical properties; for example, mercury porosimetry will not yield meaningful data if used to characterize soft materials that deform during the test and cannot be used for hydrated scaffolds.

4.5 Table 1 provides guidance for users of this guide by providing a brief overview of the applicability of a range of different measurement techniques that can be used to physically characterize tissue scaffolds. This list of techniques is not definitive.

5. Significance and Use

5.1 The ability to culture functional tissue to repair damaged or diseased tissues within the body offers a viable alternative to xenografts or heterografts. Using the patient's own cells to produce the new tissue offers significant benefits by limiting rejection by the immune system. Typically, cells harvested from the intended recipient are cultured *in vitro* using a temporary housing or scaffold. The microstructure of the scaffold, that is, its porosity, the mean size, and size distribution of pores and their interconnectivity is critical for cell migration, growth and proliferation (Appendix X1). Optimizing the design of tissue scaffolds is a complex task, given the range of available materials, different manufacturing routes, and processing conditions. All of these factors can, and will, affect the surface texture, surface chemistry, and microstructure of the resultant scaffolds. Factors that may or may not be significant variables depend on the characteristics of a given

TABLE 1 A Guide to the Physical Characterization of Tissue Scaffolds

Generic Technique	Information Available	Section
Microscopy	Pore shape, size and size distribution; porosity.	6.1 (Electron microscopy)
		6.2 (Optical microscopy)
		6.2.3 (Confocal microscopy)
		6.2.4 (Optical coherence tomography)
		6.2.5 (Optical coherence microscopy)
X-Ray micro-computed Tomography (MicroCT)	Pore shape, size and size distribution; porosity.	6.3
Magnetic Resonance Imaging	Pore shape, size and size distribution; porosity.	6.4
Measurement of density	Porosity, pore volume	7.2
Porosimetry	Porosity, total pore surface area, pore diameter, pore size distribution	7.3
Porometry	Median pore diameter (assuming cylindrical geometry), through-pore size distribution	7.4
Diffusion of markers	Permeability	8.2
NMR	Pore size and distribution	7.5

cell type at any given time (that is, changes in cell behavior due to the number of passages, mechanical stimulation, and culture conditions).

5.2 Tissue scaffolds are typically assessed using an overall value for scaffold porosity and a range of pore sizes, though the distribution of sizes is rarely quantified. Published mean pore sizes and distributions are usually obtained from electron microscopy images and quoted in the micrometer range. Tissue scaffolds are generally complex structures that are not easily interpreted in terms of pore shape and size, especially in three dimensions. Therefore, it is difficult to quantifiably assess the

batch-to-batch variance in microstructure or to make a systematic investigation of the role that the mean pore size and pore size distribution has on influencing cell behavior based solely on electron micrographs (Tomlins et al, (1)).[4]

5.2.1 Fig. 1 gives an indication of potential techniques that can be used to characterize the structure of porous tissue scaffolds and the length scale that they can measure. Clearly a

---

[4] The boldface numbers in parentheses refer to the list of references at the end of this standard.
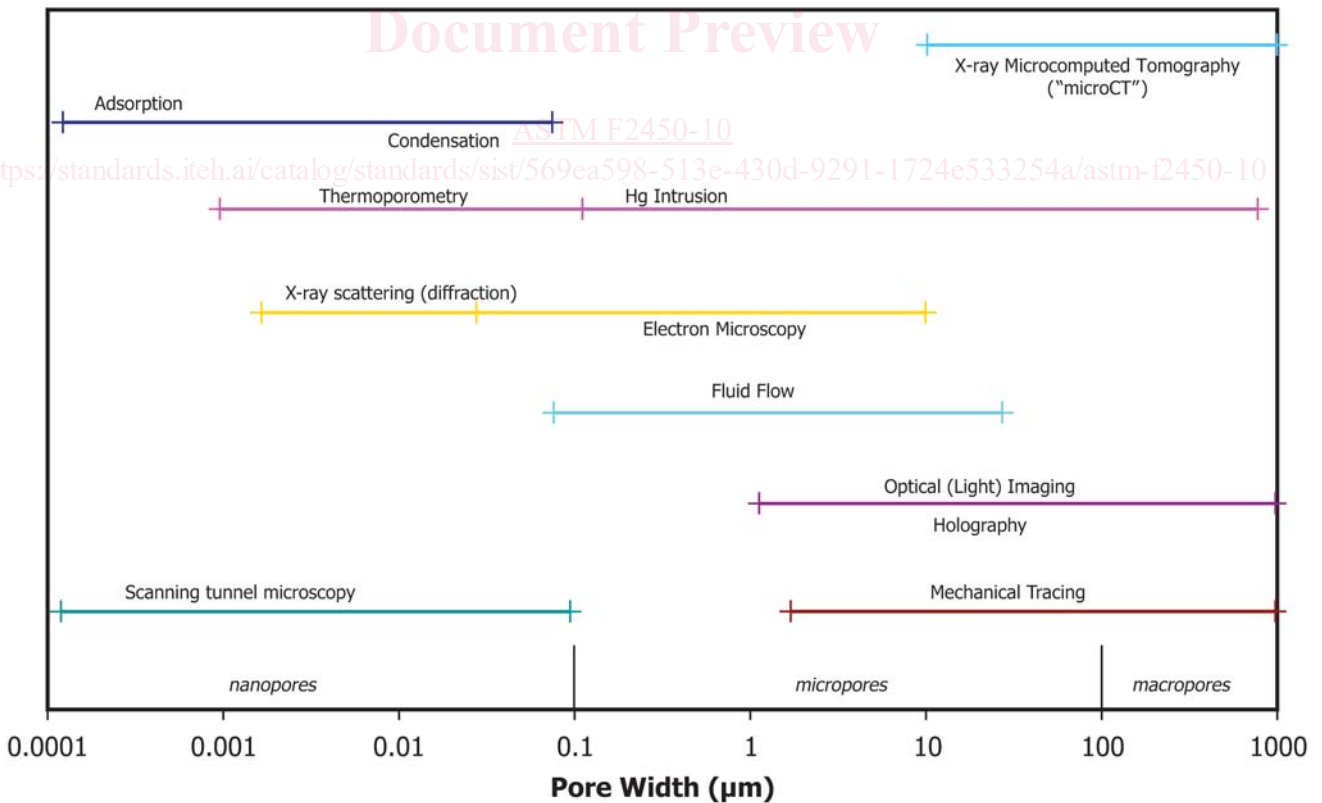
FIG. 1 A Range of Techniques is Required to Fully Characterize Porous Materials
(Note—Figure redrawn from Meyer (2).)

range of techniques must be utilized if the scaffold is to be characterized in detail.

5.2.2 The classification and terminology of pore sizes, such as those given in Table 2, has yet to be standardized, with definitions of terms varying widely (as much as three orders of magnitude) between differing applications and industries. Both Table 2 and the supporting detailed discussion included within Appendix X2 describe differences that exist between IUPAC (International Union of Pure and Applied Chemistry) definitions and the common terminology currently utilized within most life science applications, which include both implant and tissue engineering applications.

5.2.2.1 Since the literature contains many other terms for defining pores (Perret et al (3)), it is recommended that the terms used by authors to describe pores be defined in order to avoid potential confusion. Additionally, since any of the definitions in Table 2 can shift, depending on the pore size determination method (see Table 1 and Fig. 1), an accompanying statement describing the utilized assessment technique is essential.

5.2.3 All the techniques listed in Table 1 have limitations for assessing complex porous structures. Fig. 2a and Fig. 2b show a through- and a blind-end pore respectively. Porometry measurements (see 7.4) are only sensitive to the narrowest point along a variable diameter through-pore and therefore can give a lower measure of the pore diameter than other investigative techniques, such as scanning electron microscope (SEM), which may sample at a different point along the pore. The physical basis of porometry depends on the passage of gas through the material. Therefore, the technique is not sensitive to blind-end or closed pores. Therefore, estimates of porosity based on porometry data will be different from those obtained from, for example, porosimetry (see 7.3), which is sensitive to both through- and blind-pores or density determinations that can also account for through-, blind-end, *and* closed pores. The significance of these differences will depend on factors such as the percentage of the different pore types and their dimensions. Further research will enable improved guidance to be developed.

5.2.4 Polymer scaffolds range from mechanically rigid structures to soft hydrogels. The methods currently used to manufacture these structures include, but are not limited to:

5.2.4.1 Casting a polymer, dissolved in an organic solvent, over a water-soluble particulate porogen, followed by leaching.

5.2.4.2 Melt mixing of immiscible polymers followed by leaching of the water-soluble component.

5.2.4.3 Dissolution of supercritical carbon dioxide under pressure into an effectively molten polymer, a phenomenon attributed to the dramatic reduction in the glass transition temperature which occurs, followed by a reduction in pressure that leads to the formation of gas bubbles and solidification.

5.2.4.4 Controlled deposition of molten polymer to produce a well-defined three-dimensional lattice.

5.2.4.5 The manufacture of three-dimensional fibrous weaves, knits, or non-woven structures.

5.2.4.6 Chemical or ionic cross-linking of a polymeric matrix.

5.2.5 Considerations have been given to the limitations of these methods in Appendix X1.

5.2.6 This guide focuses on the specific area of characterization of polymer-based porous scaffolds and is an extension of an earlier ASTM guide, Guide F2150.

6. Imaging

6.1 *Electron Microscopy*—Both transmission and scanning electron microscopy can be used to image intact or fractured surfaces or sections cut from tissue scaffolds. The resultant images can be interpreted using image analysis software packages to generate data concerning the shape of pores within the scaffold, their mean size, and their distribution. Estimates of both permeability and tortuosity can be made from three-dimensional virtual images generated from transmission electron microscopic images of serially sectioned samples.

6.1.1 There is likely to be a high degree of uncertainty in the reliability of quantitative data derived from electron microscopic examination of soft or especially highly hydrated soft polymer-based scaffolds due to the presence of artifacts created during sample preparation. Highly hydrated scaffolds need to be freeze-dried before examination under vacuum in a conventional scanning electron microscope (SEM). This process, if carried out in liquid nitrogen, usually results in a significant amount of ice damage due to the relatively slow cooling rates that are encountered due to the thin layer of insulating nitrogen gas that forms around the sample as it is frozen. Freezing samples in slush nitrogen can reduce ice damage by enabling faster cooling rates, apparently by reducing the thickness of the insulating gas layer.

6.1.2 The relatively new technique of cryogenic SEM may also be used to reduce artifacts. In this technique, a rapidly frozen specimen can be fractured whilst frozen within the cryo-SEM unit and sputter coated with gold-palladium after allowing some of the ice to sublime away. The amount of sublimation that occurs can be controlled through exposure time. With this technique, any freeze-drying of the sample is

TABLE 2 Comparison of Pore Size Nomenclature

| Descriptor	IUPAC Definitions	Definitions for Life Science Applications
	For: chemical (for example, solid catalysts); metallurgy; geology (for example, zeolites) applications	*For: tissue engineering; medical implants; diagnostic or biological filtration applications*
Nanopore/nanoporosity	Not utilized	0.002 to 0.1 μm (2 to 100 nm)
Micropore/microporosity	<2 nm (<20 Å)	0.1 to 100 μm (typically defined 0.1 to 20 μm)
Mesopore	2 to 50 nm (20 to 500 Å)	Not utilized
Macropore/macroporosity	>50 nm (>500 Å)	>100 μm
Capillaries	Meyer, et al. (2)	Not utilized
Macrocapillaries	Meyer, et al. (2)	Not utilized
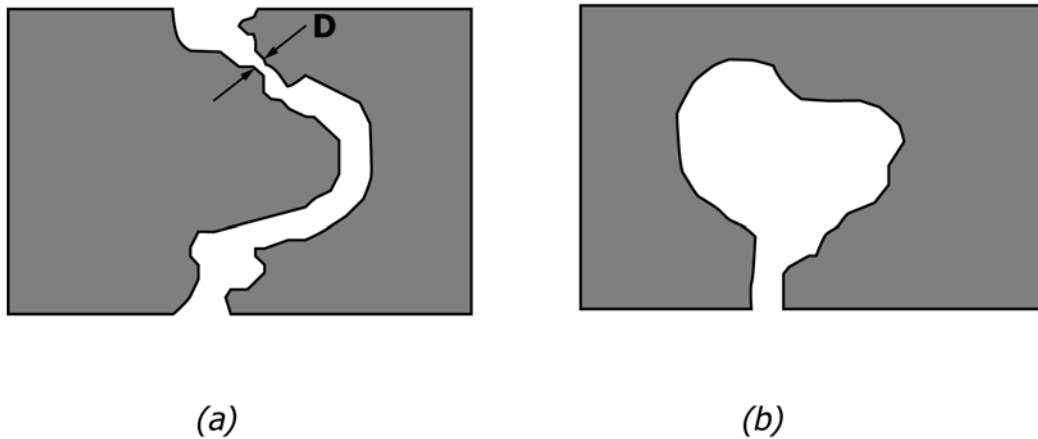
FIG. 2 A *through-pore* showing a variation of pore diameter, *D* (*a*); and an example of a *blind-pore* (*b*).

minimized. Experimentally validating the results obtained from this technique to ensure that they are artifact-free is difficult.

6.1.3 Polymer-based scaffolds often lack sufficient electron density to provide suitable levels of contrast; this can be overcome by staining using a high electron density material such as osmium tetroxide that has a high affinity for carbon-carbon double bonds.

6.1.4 Most polymer-based scaffolds can be mounted in epoxy resin using standard procedures and subsequently sectioned for serial examination in the transmission electron microscope. This method is less appropriate for investigating hydrogels that can dehydrate. However, this concern can be partially mitigated by gradual dehydration of the scaffold by using a series of alcohol solutions before embedding in resin. However, this procedure tends to reduce the size of the water-filled pores within the sample. Thus, the quantifiable pore size data subsequently obtained are of value when comparing microstructures between different samples. However, the results are less useful for characterizing expected *in vivo* microstructure due to sample distortion.

6.2 *Optical Microscopy-Based Methods:*

6.2.1 Optical methods can be utilized, providing sufficient contrast exists between the structure and surrounding media to enable surface features to be studied in a minimally prepared or natural state (that is, the specimen does not need to be stained or sectioned.) The disadvantage of this approach is that penetration of light into the sample can be limited, particularly for porous matrices, due to scattering. In practice, this limits the use of confocal microscopy and optical coherence tomography to depths that are typically less than 0.5 mm.

6.2.2 *Optical (Light) Microscopy*—Images of the surfaces of tissue scaffolds can be obtained using an optical microscope. Differential focus can used to collect images at different depths within semi-transparent specimens. These deep view images can be used to track the path of interconnected pores within the sample.

6.2.3 *Confocal Microscopy*—Substantial improvements in the quality of 'optically' sectioned samples can be made by either exploiting the natural fluorescent properties that the scaffold may have or by using a fluorescent stain such as fluorescein. Confocal microscopy can capture well-resolved images at different depths because of its shallow depth of field and elimination of out-of-focus light. A laser is usually used as a point light source in preference to a conventional lamp and in most modern instruments, several lasers are used. This capability is used to improve contrast within the image and to excite stains that bind to different structural elements and fluoresce at different wavelengths. Laser scanning confocal microscopy (LSCM) can be utilized in reflection or transmission modes. The size of the pinhole and the numerical aperture of the objective primarily determine the resolution in the thickness or axial direction. Generally, smaller holes give better resolution but at the expense of reduced intensity.

6.2.3.1 Some work on scaffold characterization using laser scanning confocal microscopy (LSCM) has been reported (Tjia and Moghe, (**4**), Birla and Matthew (**5**)).

6.2.4 *Optical Coherence Tomography*—Optical coherence tomography is a reflectance optical imaging technique that uses interferometric rejection of out-of-plane scattering of photons rather than a pinhole as in LSCM to determine axial resolution. Briefly, optical coherence tomography uses a low coherence source with a bandwidth of anywhere from 30 to 200 nm and an interferometer, usually of Michelson type, that generates profiles of back-reflected light for any one transverse position. For a complete description of optical coherence tomography and its applications, see Ref (**6**). An analogous technique is ultrasound A-scanning. In the Michelson configuration, the material is the fixed arm of the interferometer rather than a mirror. A low numerical aperture lens is used to achieve a large axial sampling volume and reflections from heterogeneities within the sample are mapped as a function of depth for any one position. Like LSCM, transverse resolution is determined by geometric optics. Unlike LSCM, axial resolution is inversely proportional to the bandwidth of the source, and a typical value for axial resolution is 10 mm.

6.2.4.1 The advantage of optical coherence tomography is that it is highly sensitive, typically 90 dB. Optical coherence tomography has been extensively used to image the human retina (Hee et al (**7**)), skin and blood vessels (Barton et al (**8**)), and the functioning circulatory systems of small live animals (Boppart et al (**9**)) with excellent clarity. In the late 1990s, the

potential for optical coherence tomography in the area of materials science was first seen. The first published optical coherence tomography images of a tissue-engineering scaffold were of a hydrogel and demonstrated the depth to which images can be obtained (McDonough et al (**10**)). The depth of field of the image is limited by scattering from the pores and any crystallites that are present. It can vary from approximately 100 μm to several millimetres depending on the difference in refractive index between the material and its surroundings, the level of porosity, and the pore size distribution. The penetration depth can be improved by filling the pores with a fluid of similar refractive index to the scaffold material. In practice, this is usually a substitution of water for air or oil for water. This procedure can result in additional problems due to poor wetting and trapped air. Optical coherence tomography images of porous materials tend to be noisy due to multiply scattered photons that contribute to the signal. A related technique, optical coherence microscopy, overcomes the issues related to the fidelity of imaging tissue-engineering scaffolds.

6.2.5 *Optical Coherence Microscopy*—Optical coherence microscopy is a combination of optical coherence tomography and confocal microscopy. Optical coherence microscopy is highly suited for imaging of optically opaque materials such as tissue-engineering scaffolds because it can attain axial and transverse resolution on the order of a micrometer and still maintain high background rejection. The confocal enhancement is done in the usual manner by the addition of a high numerical aperture objective and a pinhole, which is usually the open aperture of the sample arm fiber. For more information on optical coherence microscopy, see Ref (**6**). The key to the technique is the axial point spread functions (PSF) of the confocal and coherence techniques. For the confocal component, the Lorentzian axial PSF results in a finite collection efficiency even far out of the focus plane, and this limits its use in highly scattering media such as TEMPs. For the coherence component, the Gaussian PSF drops off far from the focal plane much more rapidly than that of confocal microscopy. Hence, the confocal component contributes to the high resolution near the focus and the coherence component contributes to the high background rejection, two qualities needed for effective imaging of TEMPs (Dunkers et al (**11**)).

6.3 *X-Ray Micro-computed Tomography (MicroCT)*—X-rays can be used to generate three-dimensional images of tissue scaffolds from which information on pore size and shape, porosity, and interconnectivity can be obtained. The principle of the method is to position the scaffold between an X-ray source and a detector. The sample is rotated and the X-ray attenuation is recorded at a number of different angles. These data can then be analyzed using reconstruction algorithms to produce an image of a two-dimensional slice through the scaffold. A full three-dimensional image can be generated from a series of two-dimensional slices obtained at different heights within the sample. Typical resolution of such an image is around 5 to 10 μm, but instruments that can resolve 50 nm are now commercially available. The success of the technique relies on there being sufficient contrast, that is, differences in electron density between the solid material and a fluid (typically air or water) within the pores.

6.3.1 The technique does not suffer from the same penetration depth limitations that optical tomographic methods suffer from, providing a more complete picture of the scaffold structure. Further information can be found in Guide E1441. The non-destructive approach has been used to investigate the structure of bone and other materials (Muller et al, (**12**), Muller et al, (**13**)) to validate the design of bone scaffolds (Van Oosterwijck et al, (**14**)) and to investigate polymeric scaffolds (Maspero et al (**15**), Lin et al (**16**)).

6.4 *Magnetic Resonance Imaging*—Many polymers contain magnetic resonance (MR) active nuclei (for example, 1H, 13C), but the relaxation times of nuclei on the polymer backbone are too short for routine imaging applications. Thus, to study the three-dimensional morphology of polymeric scaffolds, the pore space must be filled with a fluid, which is visible in a magnetic resonance imaging (MRI) experiment. The ideal fluid must contain MR active nuclei, which are naturally abundant, have a high receptivity, and have a well-resolved nuclear magnetic resonance (NMR) spectrum of narrow lines. Moreover, it needs to have a low viscosity to infiltrate the pore space and must have appropriate relaxation properties to provide a large signal, after the application of the imaging gradients. Fortunately, immersion in water will suffice for most polymeric scaffolds.

6.4.1 The theoretical limit in spatial resolution for MRI experiments is typically the distance (~10 μm) a water molecule diffuses during the time it takes to acquire the MRI signal. Thus, polymeric scaffolds with large pores (50 to 100 μm) can be spatially resolved with this technique. In MR images, the water-filled pores appear bright and the polymer mesh dark. High contrast images of the polymer mesh, after suitable image analysis, can be used to generate estimates of pore sizes and pore size distribution.

6.4.2 The porosity of scaffolds that have pores that are smaller than the resolution limit of the MRI technique can be estimated from the signal intensity of a water-saturated scaffold normalized to that of pure water. The normalized signal intensity reflects the volume fraction of water present within the polymer scaffold, if the polymer does not contribute to the measured signal. For hydrogels, a better estimate of the polymeric volume fraction can be derived from quantitative transverse relaxation maps. This approach is used to analyze the density of cross-links in hydrogels used as radiation dosimetry phantoms. For polymeric scaffolds with pore sizes comparable to the diameter of a cell (10 to 20 μm), MR images of the diffusion behaviour of the pore fluid can yield estimates of the pore size and size distribution. A limitation of this approach is the need to assume a geometric model to obtain structural information.

6.4.3 Other limitations of the MRI technique include its low spatial resolution and the necessity of a pore fluid to study the structure of the scaffold, which limits the technique to detecting only those pores that are fluid-filled. In practice, MRI will be unable to detect enclosed pores or those which either trap air (blind-end pores) or are difficult to wet out due to surface tension. The distribution of the pore fluid within the scaffold is